© 2014. Published by The Company of Biologists Ltd | Journal of Cell Science (2014) 127, 4494–4506 doi:10.1242/jcs.155523

RESEARCH ARTICLE

Secreted fibroblast-derived miR-34a induces tubular cell apoptosis in fibrotic kidney

Yang Zhou[1,*], Mingxia Xiong[1,*], Jing Niu[1], Qi Sun[1], Weifang Su[1], Ke Zen[2], Chunsun Dai[1,‡] and Junwei Yang[1,‡]

ABSTRACT

Tubular epithelial cell apoptosis contributes to tubulointerstitial fibrosis but its regulation remains unclear. Here, in fibrotic kidney induced by unilateral ureteral obstruction (UUO), we demonstrate that miR-34a is markedly upregulated in tubulointerstitial spaces and microvesicles isolated from obstructed kidney. However, miR-34a is not *de novo* synthesized by proximal tubular epithelial cells but by fibroblasts after incubation with TGF-β1. miR-34a is markedly upregulated in microvesicles isolated from the cell culture medium of TGF-β1-treated fibroblasts. These microvesicles act as a vector for delivery of upregulated miR-34a from fibroblasts to tubular cells. The fibroblast-derived miR-34a-containing microvesicles induce the apoptosis of tubular cells. The exogenous miR-34a regulates tubular apoptosis by modulating the expression of the anti-apoptotic protein Bcl-2. Moreover, injection of exogenous miR-34a-containing microvesicles enhances tubular cell apoptosis in mice. This study suggests that secreted fibroblast miR-34a transported by microvesicles induces tubular cell apoptosis in obstructed kidney. This study reveals a new mechanism whereby microvesicle-mediated communication of miRNA between fibroblasts and tubular cells is involved in regulating tubular cell apoptosis, which might provide new therapeutic targets for renal tubulointerstitial fibrosis.

KEY WORDS: Apoptosis, miRNA, Microvesicle, miR-34a, Kidney fibrosis

INTRODUCTION

Renal fibrosis involves tubular atrophy and extracellular matrix accumulation in the tubulointerstitial spaces (Bohle et al., 1979). Apoptosis contributes to tubular atrophy (Johnson and DiPietro, 2013) and is one of the mechanisms of progressive tubulointerstitial fibrosis (Docherty et al., 2006; Liu, 2004). The evidence for apoptosis in obstructed kidney was provided by immunohistochemical detection of apoptotic markers and histochemical detection of DNA breaks [by terminal deoxynucleotidyl transferase dUTP nick end labeling (TUNEL)] in previous investigations (Zhang et al., 2001). Stimuli in obstructed kidney, such as hypoxia, oxidative stress and particularly TGF-β1 (Dai et al., 2003; Miyajima et al., 2000) are the common causes of apoptosis, which promotes an inflammatory response and results in matrix synthesis and deposition by parenchymal renal cells and, ultimately, renal fibrosis (Docherty et al., 2006). Moreover, therapies that ameliorate apoptosis, such as treatment with hepatic growth factor (Gao et al., 2002; Liu, 2004; Mizuno et al., 2001), bone morphogenetic protein-7 (Morrissey et al., 2002) and angiotensin receptor blocker (Kellner et al., 2006) prevent the progression of fibrosis.

Apoptosis is a programmed cell death that occurs in multicellular organisms. In addition to its importance as a biological phenomenon, apoptosis has been implicated in an extensive variety of diseases. The process of apoptosis is controlled by a diverse range of cell signals. In cancer studies, it has been demonstrated that the transcription of the microRNA (miR)-34 family, including miR-34a, miR-34b and miR-34c, is directly induced by p53, a tumor suppressor gene (Hermeking, 2010). Loss of miR-34a has been identified in cell lines of most tumors (Lodygin et al., 2008). In addition, the absence of miR-34 expression has been linked to resistance to apoptosis induced by p53-activating agents used in chemotherapy (Kumamoto et al., 2008). Among the miR-34 family, miR-34a is widely expressed in mammalian tissues. Here, we examine whether miR-34a regulates cell apoptosis in the progression of fibrosis. Microvesicles are small vesicles that are shed from almost all cell types under physiological and pathological conditions (Cocucci et al., 2008; Théry et al., 2002). Microvesicles carrying mRNA and miRNA are reported to mediate cell-to-cell communication between renal parenchymal cells to promote fibrosis (Borges et al., 2013; Zhou et al., 2013). The microvesicles are perfect vectors of signals because the encapsulation of protein, mRNA and miRNA within a lipid bilayer protects them from degradation. The apoptosis repressor and survival factor Bcl-2 is transcriptionally regulated by p53 (Budhram-Mahadeo et al., 1999), and the 3′ untranslated region (UTR) of Bcl-2 is targeted by miR-34a (Bommer et al., 2007). It has been reported that miR-34a-defective cells show a decrease in spontaneous apoptosis (Bommer et al., 2007). The regulation of Bcl-2 by miR-34a and its effects on apoptosis were therefore evaluated in renal fibrosis.

In this study, it was found that miR-34a is upregulated in injured fibroblasts, is then secreted and is delivered into tubular epithelial cells through disrupted tubular basement membrane (TBM) by microvesicles. This study highlights the importance of cell-to-cell communication in the progression of renal fibrosis, demonstrates a new mechanism concerning apoptosis in fibrosis and will probably provide therapeutic targets for renal fibrosis.

RESULTS

MiR-34a is upregulated in obstructed kidney and in microvesicles isolated from obstructed kidney

Cell apoptosis was evident in a mouse model of renal fibrosis induced by obstruction, as revealed by TUNEL staining (supplementary material Fig. S1). As shown in supplementary material Fig. S1B,D, the TUNEL-positive cells (brown nuclei)

[1]Center for Kidney Disease, 2nd Affiliated Hospital, Nanjing Medical University, 262 North Zhongshan Road, Nanjing, Jiangsu 210003, China. [2]Jiangsu Engineering Research Center for MicroRNA Biology and Biotechnology, School of Life Sciences, Nanjing University, 22 Hankou Road, Nanjing, Jiangsu 210093, China.
*These authors contributed equally to this work

‡Authors for correspondence (daichunsun@njmu.edu.cn; jwyang@njmu.edu.cn)

Received 21 April 2014; Accepted 29 July 2014

Journal of Cell Science

Journal of Cell Science (2014) 127, 4494–4506 doi:10.1242/jcs.155523

were probably tubular cells, which became hard to identify owing to the deterioration of renal morphology after kidney obstruction (supplementary material Fig. S1E). The detached apoptotic tubular cells were probably shed into the lumens and discarded with the urine (supplementary material Fig. S1G,H). Previous investigations have shown that miR-34a regulates apoptosis in tumor cells; we therefore examined miR-34a expression in obstructed kidney by *in situ* hybridization (ISH) and quantitative (Q)-PCR. As shown in Fig. 1A–F, the expression of miR-34a was markedly increased in obstructed kidney (Fig. 1B–E, purple-staining cells), predominantly in tubular cells (arrows); however, at 1 day after obstruction, some interstitial cells were also miR-34a-positive (Fig. 1F, arrow). In accordance with the morphological results, quantification of miR-34a expression levels in whole kidney tissue by Q-PCR analysis revealed that miR-34a was upregulated as early as day 1 and remained upregulated until day 14, reaching peak expression levels at around day 3 to day 7 after obstruction (Fig. 1G). To determine whether miR-34a was upregulated in apoptotic cells and induced cell detachment, we collected the urine in the pelvis of the obstructed kidney and examined its miR-34a expression level. As expected, the excretion of miR-34a was dramatically upregulated after kidney obstruction (Fig. 1H). The dynamic changes in excretion levels of miR-34a in obstructed urine were in accordance with expression levels of miR-34a in the obstructed kidney; however, the fold increase seemed amazingly high. It is probable that miR-34a in the urine is present in cell debris or apoptotic cells that detached from the obstructed kidney and were excreted into urine.

To determine whether miR-34a was secreted, the microvesicles in the kidney cortex of sham and UUO mice at 7 days after obstruction were isolated. Under the electron microscope, the isolated microvesicles from obstructed kidney appeared as clusters of vesicles of ~30–200 nm in diameter (Fig. 1I), surrounded by a double-layer membrane (Fig. 1J). Total RNA was isolated from microvesicles containing 1 mg of microvesicle protein. The relative abundance of miR-34a was evaluated by Q-PCR. As shown in Fig. 1K, the miR-34a level in microvesicles isolated from obstructed kidney was markedly upregulated. This suggested that the content of miR-34a in each microvesicle was probably upregulated after obstruction. Expression of CD63 indicated that the pellets from the kidney cortex after ultracentrifugation were microvesicles (Fig. 1L). Because protein extracts prepared from kidney microvesicles were normalized to kidney tissue protein (actin) and the size of microvesicles are within the same range, the upregulated CD63 indicated that obstructed kidneys produced more microvesicles.

Expression of miR-34a is upregulated in TGF-β1-treated fibroblasts

ISH analysis revealed that miR-34a was upregulated in both tubular and interstitial cells of obstructed kidney. We further

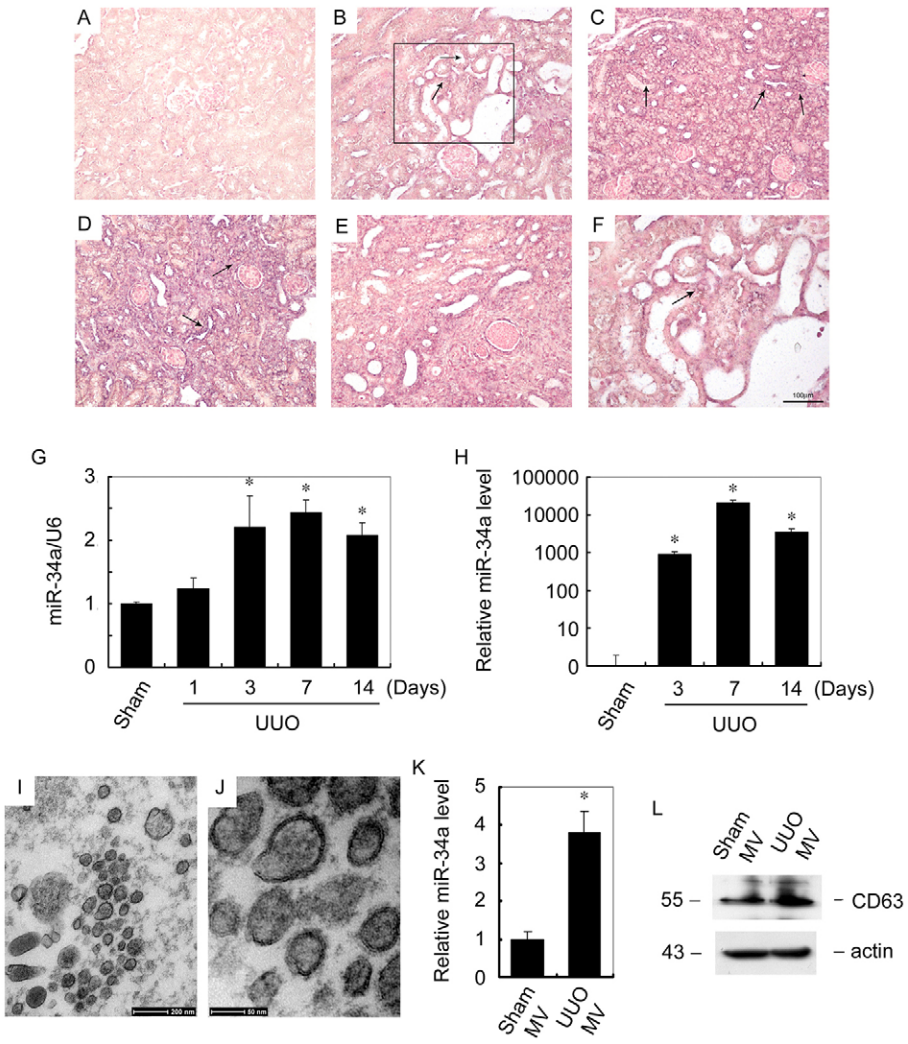

Fig. 1. miR-34a is upregulated in obstructed kidney and in microvesicles isolated from obstructive kidney. (A–F) Representative images show the ISH analysis of mature miR-34a in kidney. (A) Sham. (B) 1 day after UUO. (C) 3 days after UUO. (D) 7 days after UUO. (E) 14 days after UUO. (F) A magnified image of the area outlined in black in B. Arrows point to miR-34a-positive tubulointerstitial cells (purple staining). Scale bars: 100 μm. (G) Q-PCR analysis of the relative expression levels of miR-34a in UUO versus sham kidneys. (H) Total RNA was isolated from 200 μl of urine using acidic phenol. Q-PCR analysis of relative expression levels of miR-34a in urine from UUO or sham kidneys is shown. (I) TEM micrograph of microvesicles isolated from obstructed mouse kidney. Scale bar: 200 nm. (J) TEM micrograph of microvesicles isolated from obstructed mouse kidney. Scale bar: 50 nm. (K) Microvesicles (MV) were isolated from the kidney cortex of sham and 7 day UUO mice. Protein concentrations of isolated microvesicles were normalized. Q-PCR analysis of the relative amount of miR-34a in microvesicle samples that contained 1 mg of microvesicle protein is shown. For G,H and K, data show the mean±s.e.m. (n=5); *P<0.05 versus sham. (L) Western blot analysis of the amount of CD63 protein in isolated microvesicles. Protein extracts prepared from kidney microvesicles are normalized to kidney tissue protein level (actin).

Journal of Cell Science (2014) 127, 4494–4506 doi:10.1242/jcs.155523

examined the expression of miR-34a by Q-PCR analysis in cultured tubular cells (NRK-52E) and fibroblasts (NRK-49F) after TGF-β1 treatment. As shown in Fig. 2A, the expression of miR-34a in TGF-β1-treated tubular cells was not significantly upregulated, despite a weak tendency towards an increase in expression. However, in cultured fibroblasts, the expression of miR-34a was markedly upregulated by incubation with 5 ng/ml TGF-β1 (Fig. 2B). As compared with control cells, the expression of miR-34a in fibroblasts reached a threefold upregulation after treatment with TGF-β1, and the increase started as early as 1 hour after treatment and lasted for the initial 4 hours. Fig. 4C shows that upregulation of miR-34a in fibroblasts induced by TGF-β1 treatment was abolished by pre-transfection of the cells with a miR-34a inhibitor. Because of the transportability of miRNA that has been reported previously (Camussi et al., 2010; Zhang et al., 2010; Zhou et al., 2013), we hypothesized that miR-34a might be upregulated in fibroblasts, then secreted and delivered to adjacent tubular cells. In normal kidney, under physiological conditions, tubular cells and fibroblasts are separated by the TBM; however, in fibrotic kidney, TBM disruption was evident (Fig. 2D–H,

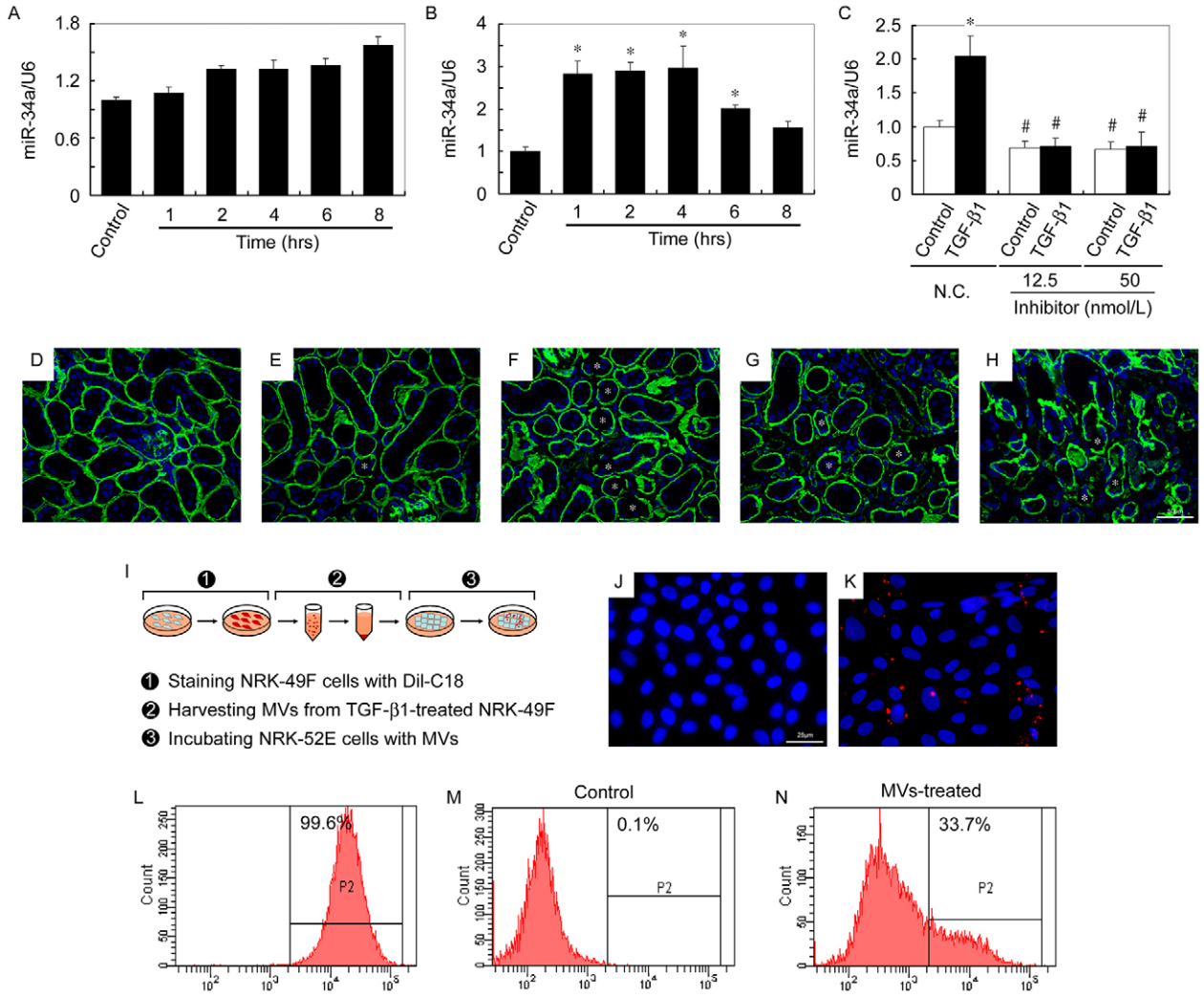

Fig. 2. Microvesicles from TGF-β1-treated fibroblasts can be transported into cultured tubular cells. (A) Q-PCR analysis of the relative expression levels of miR-34a in NRK-52E cells after incubation with 5 ng/ml TGF-β1 for various time-periods as indicated. (B) Q-PCR analysis of the relative expression levels of miR-34a in NRK-49F cells after incubation with 5 ng/ml TGF-β1 for various time-periods as indicated. (C) NRK-49F cells were transfected with the miR-34a inhibitor at various concentrations as indicated and then incubated with TGF-β1 for 6 hours. Q-PCR analysis of relative expression levels of miR-34a in NRK-49F cells. Data in A–C show the mean±s.e.m. (n=3); *P<0.05 versus control; $^{\#}P$<0.05 versus corresponding cells transfected with negative control (N.C.). (D–H) Representative images showing the immunofluorescent staining of laminin in kidney. (D) Sham. (E) 1 day after UUO. (F) 3 days after UUO. (G) 7 days after UUO. (H) 14 days after UUO. Green, laminin; blue, nuclei; asterisks mark disrupted TBM. Images are shown under 400× magnification. Scale bars: 50 μm. (I) Schematic depiction of the experiment evaluating the transportability of microvesicles (MVs) from fibroblasts to tubular cells. (J,K) Fluorescent staining illustrates the intercellular transfer of microvesicles. TGF-β1-treated NRK-49F cells were labeled with or without (control) DiI-C18 (red). The culture media were collected and centrifuged to harvest microvesicles. The microvesicles were resuspended in medium and incubated with NRK-52E cells at 37˚C. After incubation for 12 hours, NRK-52E cells were washed, fixed and observed by microscopy. (J) NRK-52E cells with control microvesicles. (K) NRK-52E cells with DiI-C18-labeled microvesicles. Scale bars: 25 μm. (L) NRK-49F cells stained with DiI-C18 were analyzed on a flow cytometer (n=3). (M) Microvesicles were isolated from TGF-β1-treated NRK-49F cells (unstained, control) and applied to NRK-52E cells for 12 hours. These NRK-52E cells were then analyzed on a flow cytometer as a control. (N) Microvesicles were isolated from DiI-C18-pre-stained and TGF-β1-treated NRK-49F cells and applied to NRK-52E cells for 12 hours. NRK-52E cells were then analyzed on a flow cytometer (n=3).

Journal of Cell Science (2014) 127, 4494–4506 doi:10.1242/jcs.155523

asterisks), which could provide a mechanism to facilitate the delivery of miR-34a from fibroblasts to tubular cells.

Microvesicles from fibroblasts can be transported into cultured tubular cells

Microvesicles are a commonly accepted vector of miRNA. We therefore examined whether fibroblast-derived microvesicles could be transported into cultured tubular cells. Fig. 2I shows a schematic illustration of the experimental protocol. Cell membranes of cultured fibroblasts were marked with a fluorescent stain named Dil-C18, which efficiently labeled >99% of the cultured fibroblasts (Fig. 2L). Microvesicles harvested from TGF-β1-treated fibroblasts were collected by differential centrifugation. These microvesicles carried part of the membrane of fibroblasts and were consequently Dil-C18-positive. Fig. 2K shows Dil-C18-positive dots in the recipient NRK-52E cells incubated with Dil-C18-labeled microvesicles. Fig. 2N shows that after a 12-hour incubation with Dil-C18-positive microvesicles isolated from fibroblasts, >30% of tubular cells were stained with Dil-C18, which suggests the transportability of microvesicles from fibroblasts to cultured tubular cells.

Secreted fibroblast miR-34a induces apoptosis in cultured tubular cells

Disrupted TBM in fibrotic kidney and microvesicles that can be transported from fibroblasts to tubular cells provide the route and means of transport for the delivery of miR-34a. We next determined whether miR-34a was transported in microvesicles. To determine whether miR-34a was secreted, microvesicles were collected from the cell culture medium of fibroblasts with or without TGF-β1 treatment. Total RNA was isolated from microvesicles containing 1 mg of microvesicle protein. The relative abundance of miR-34a was evaluated by Q-PCR. Fig. 3A shows an eightfold increase in miR-34a expression level in microvesicles of TGF-β1-treated fibroblasts. This result suggests that the miR-34a content of each fibroblast microvesicle was upregulated after TGF-β1 treatment. Expression of CD63 indicated that the pellets from cell culture medium after ultracentrifugation were microvesicles (Fig. 3B). Protein extracts prepared from fibroblast microvesicles were normalized to cell protein (actin), the upregulated CD63 indicated that TGF-β1-incubated fibroblasts produced more microvesicles. Pre-transfection with a miR-34a inhibitor reduced the miR-34a level in microvesicles from TGF-β1-treated fibroblasts (Fig. 3C). Taken together, these results show that TGF-β1 induced upregulation of miR-34a in fibroblasts, and miR-34a was secreted by way of microvesicles. The microvesicles collected from TGF-β1-treated fibroblasts were then applied to cultured tubular cells. As shown in Fig. 3D, after being treated with these microvesicles [which were shown above to be transportable between cultured fibroblasts and tubular cells (Fig. 2)] from fibroblasts for 12 h, miR-34a in the recipient cultured tubular cells was markedly upregulated. As we expected, miR-34a in tubular cells was not upregulated by microvesicles from fibroblasts that were pre-transfected with the miR-34a inhibitor and then treated with TGF-β1 (Fig. 3D). Moreover, the pre-miR-34a level in tubular cells was not changed by fibroblast microvesicles, which suggests that upregulated miR-34a in tubular cells was exogenous (supplementary material Fig. S2). We conclude that miR-34a was ultimately delivered into target tubular cells. The steps might be as follows; miR-34a is upregulated in fibroblasts, secreted in microvesicles, delivered through the disrupted TBM and transported into tubular cells. Microvesicles act as an important vector in this process. Furthermore, the annexin-V–FITC assay and TUNEL staining, which detect the initial and advanced stage of apoptosis, respectively, were applied to examine the effect of microvesicles on apoptosis of recipient tubular cells. As shown in Fig. 3E–I, the percentage of annexin-V-positive cells and TUNEL-positive cells were both increased after incubation with microvesicles from TGF-β1-treated fibroblasts. These results suggest that secreted microvesicles from TGF-β1-treated fibroblasts induce apoptosis of recipient tubular cells.

miR-34a regulates apoptosis of tubular cells

The effect of miR-34a on apoptosis of tubular cells was then evaluated. miR-34a levels were modulated by transfection of mimic or inhibitor. Fig. 4A shows that the miR-34a level in tubular cells was markedly downregulated by the miR-34a inhibitor. Meanwhile, miR-34a level in tubular cells was markedly upregulated by the miR-34a mimic (Fig. 4B). These results verified the efficiency of modulation of miR-34a expression levels by transfection of mimic or inhibitor in cultured tubular cells. We then used the annexin-V–FITC assay and TUNEL staining to compare apoptosis between tubular cells transfected with negative control and 50nmol/l of mimic or inhibitor. As shown in Fig. 4C,D, the percentage of annexin-V-positive cells was markedly upregulated by the miR-34a mimic. Fig. 4E–H show that the percentage of TUNEL-positive cells was markedly upregulated by miR-34a mimic and downregulated by the miR-34a inhibitor. Taken together, these results show that overexpression of miR-34a promoted both the initial and advanced stage of apoptosis and that suppression of miR-34a inhibited the advanced stage of apoptosis in cultured tubular cells.

miR-34a targets anti-apoptotic Bcl-2 in tubular cells

To determine the target of miR-34a, we used TargetScan and found that Bcl-2, an anti-apoptotic protein, was the predicted target of miR-34a. Fig. 5A shows that luciferase activities were decreased and increased in the presence of miR-34a and anti-miR-34a, respectively, and these effects were abolished when the miR-34a-binding site of Bcl-2 (3′UTR) was mutated. In tubular cells, the mRNA level of Bcl-2 was upregulated by the miR-34a inhibitor and downregulated by the miR-34a mimic (Fig. 5B). Fig. 5C,D show that the protein level of Bcl-2 was also upregulated by the miR-34a inhibitor and downregulated by the miR-34a mimic. These results suggest that miR-34a regulates the transcription of Bcl-2, and therefore affects the mRNA and protein levels of Bcl-2 in tubular cells. Furthermore, the effects of microvesicles on Bcl-2 expression in tubular cells were examined. As shown in Fig. 5E–G, after incubating with microvesicles from TGF-β1-treated fibroblasts, the mRNA and protein levels of Bcl-2 were both downregulated.

Downregulation of Bcl-2 results in apoptosis of tubular cells

Transfection of specific siRNA downregulates mRNA (Fig. 6A) and protein (Fig. 6B,C) levels of Bcl-2 in tubular cells. Fig. 6D shows that the percentage of apoptotic cells was upregulated dose-dependently by Bcl-2 siRNA. Transfection of a medium dose (50 nmol/l) of Bcl-2 siRNA resulted in a twofold increase in cell apoptosis; however, the percentage of both apoptotic (annexin-V-positive) and necrotic (annexin-V-positive and propidium-iodide-positive) cells was markedly increased by a large dose (100 nmol/l) of Bcl-2 siRNA (Fig. 6D). Fig. 6E–I

Journal of Cell Science (2014) 127, 4494–4506 doi:10.1242/jcs.155523

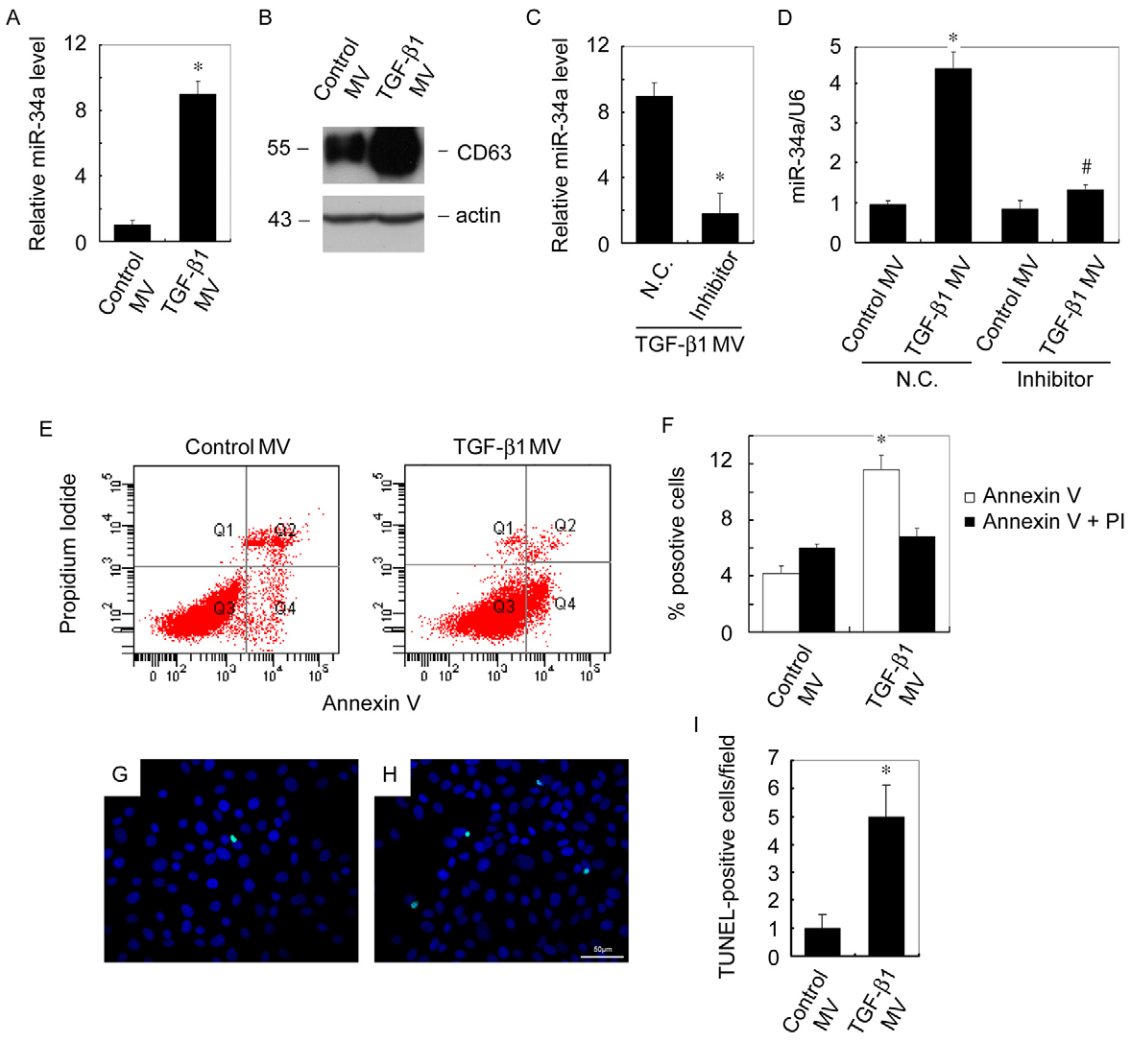

Fig. 3. Secreted fibroblast miR-34a induces apoptosis in cultured tubular cells. (A) Microvesicles (MV) were isolated from the cell culture media of NRK-49F cells that has been incubated without (control MV) or with 5 ng/ml of TGF-β1 (TGF-β1 MV) for 48 hours. Protein concentrations of isolated microvesicles were normalized. Q-PCR analysis of the relative miR-34a amount in microvesicle samples that contained 1 mg of microvesicle protein. (B) Western blot analysis of the amount of CD63 protein in isolated microvesicles. Protein extracts prepared from fibroblast microvesicles were normalized to cell protein level (actin). (C) NRK-49F cells were transfected with miR-34a inhibitor or its negative control (N.C.) and then incubated with TGF-β1 for 48 hours. Q-PCR analysis of the relative expression levels of miR-34a in microvesicles isolated from culture media of these NRK-49F cells. (D) NRK-52E cells were incubated with microvesicles isolated from NRK-49F cells pre-transfected with N.C. or miR-34a inhibitor and then treated without (control MV) or with TGF-β1 (TGF-β1 MV). After incubation for 12 hours, Q-PCR analysis of the relative expression levels of miR-34a in these NRK-52E cells was performed. (E) Apoptosis of NRK-52E cells incubated with control MV or TGF-β1 MV was analyzed by annexin V/propidium iodide (PI) staining on a flow cytometer. (F) The percentage of positive cells analyzed by flow cytometry is shown. (G,H) Representative images show the apoptosis of NRK-52E cells incubated with control MV or TGF-β1 MV as analyzed by TUNEL staining. (G) Control MV. (H) TGF-β1 MV. Scale bars: 50 μm. (I) The percentage of positive cells as determined by TUNEL staining is shown. Data in A,C,D,F,I show the mean±s.e.m. (n=3); *P<0.05 versus control (A,D,F,I) or versus N.C. (D); $^{\#}P$<0.05 versus corresponding cells transfected with N.C. (D).

show that the number of TUNEL-positive cells was dose-dependently increased by Bcl-2 siRNA. Taken together, these results show that downregulation of Bcl-2 in tubular cells by RNA interference induced cell apoptosis, which indicated that Bcl-2 was an anti-apoptotic protein in tubular cells.

miR-34a regulates tubular cell apoptosis by targeting Bcl-2

To determine whether Bcl-2 was indispensable for the regulation of cell apoptosis by miR-34a, tubular cells were co-transfected with miR-34a inhibitor and Bcl-2 siRNA. miR-34a was downregulated by the miR-34a inhibitor with or without the presence of Bcl-2 siRNA (Fig. 7A). The transcription of Bcl-2 was derepressed by the miR-34a inhibitor; however, the upregulation of Bcl-2 that was induced by the miR-34a inhibitor was abolished by co-transfection with Bcl-2 siRNA (Fig. 7B). Fig. 7C,D show that the upregulation of Bcl-2 protein by the miR-34a inhibitor was eliminated by treatment with Bcl-2 siRNA. Fig. 7E–K show that repression of cell apoptosis by the miR-34a inhibitor was diminished by transfecting cells with Bcl-2 siRNA. Moreover, Bcl-2 inhibition resulted in an increase in cell apoptosis with or without the presence of miR-34a inhibitor. Taken together, these results show that the anti-apoptotic effect of

Journal of Cell Science (2014) 127, 4494–4506 doi:10.1242/jcs.155523

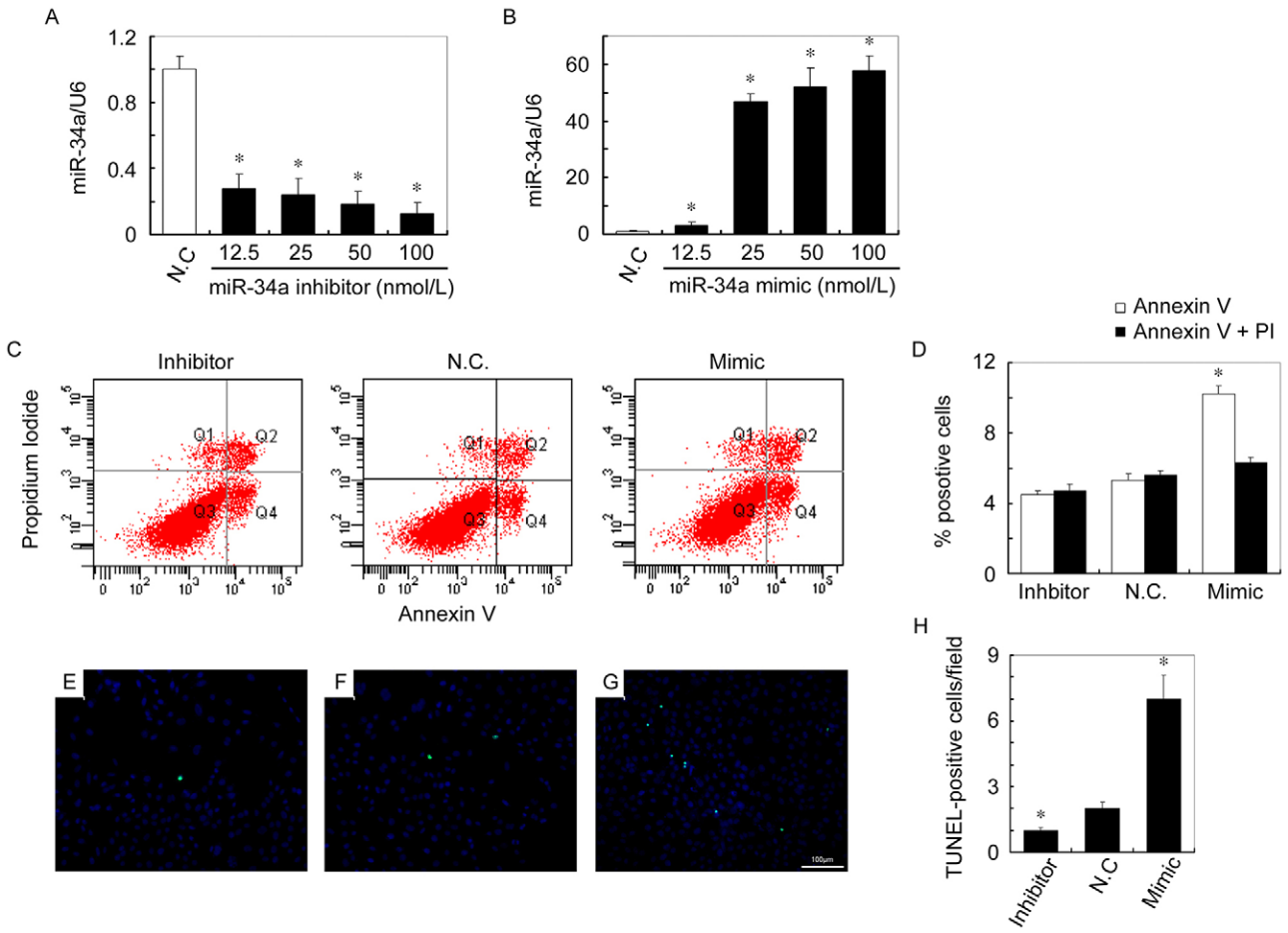

Fig. 4. miR-34a regulates apoptosis of tubular cells. (A) Q-PCR analysis of the relative expression levels of miR-34a in NRK-52E cells transfected with different doses of miR-34a inhibitor as indicated. (B) Q-PCR analysis of the relative expression levels of miR-34a in NRK-52E cells transfected with different doses of miR-34a mimic as indicated. (C) Apoptosis of NRK-52E cells transfected with miR-34a inhibitor, miR-34a mimic or negative control (N.C.) at a dose of 50 nmol/l was analyzed by annexin V/propidium iodide (PI) staining, using a flow cytometer. (D) Graphic representation of the percentage of positive cells as determined by flow cytometry. (E–G) Representative images show the apoptosis of NRK-52E cells transfected with miR-34a inhibitor, miR-34a mimic or negative control at a dose of 50 nmol/l, as determined by using TUNEL staining. (E) miR-34a inhibitor. (F) Negative control. (G) miR-34a mimic. Scale bars: 100 μm. (H) Graphic representation of the percentage of positive cells as determined by TUNEL staining. For A,B,D and H, data show the mean±s.e.m. (n=3); *P<0.05 versus N.C.

the miR-34a inhibitor is dependent on miR-34a-inhibitor-induced upregulation of Bcl-2 expression.

Exogenous miR-34a-containing microvesicles from TGF-β1-treated fibroblasts enhance tubular cell apoptosis

The observation that secreted fibroblast miR-34a can induce tubular cell apoptosis was further confirmed in mouse kidney. Dil-C18-labeled microvesicles isolated from TGF-β1-treated fibroblasts were intravenously injected into CD-1 mice, and the kidney of mice was harvested and viewed by fluorescence microscopy. Fig. 8A shows that mouse kidney was fluorescently labeled (red dots, arrows) at 1 day post-injection. According to the characteristics of blood circulation and distributions, a majority of microvesicles were trapped in liver and lung (supplementary material Fig. S3). Q-PCR analysis revealed that miR-34a was upregulated in mouse kidney, whereas the injection of microvesicles from control fibroblasts had no effect on miR-34a expression (Fig. 8B). However, the level of pre-miR-34a in mouse kidney was not changed by fibroblast microvesicles, which suggests that the upregulation of miR-34a was due to microvesicle-mediated delivery of exogenous miRNA (supplementary material Fig. S4). Fig. 8C shows that the mRNA levels of Bcl-2 in mouse kidney injected with TGF-β1 microvesicles were consequently downregulated. Fig. 8D–G (arrow) show that the number of TUNEL-positive cells (brown nuclei) was upregulated after injection of TGF-β1 microvesicles. Most of the TUNEL-positive cells were tubular cells. Taken together, these data reveal that the upregulation of miR-34a by intravenous injection of exogenous miR-34a-containing microvesicles induced tubular cell apoptosis.

DISCUSSION

It was found in this study that miR-34a is upregulated in injured fibroblasts in obstructed kidney and is then secreted and delivered into tubular epithelial cells by microvesicles through the disrupted TBM. The transported miR-34a then induces tubular cell apoptosis by targeting anti-apoptotic Bcl-2. This study highlights the mechanism of microvesicle-mediated fibroblast-to-tubular cell communication in the pathogenesis of renal fibrosis and might provide novel therapeutic targets.

Journal of Cell Science (2014) 127, 4494–4506 doi:10.1242/jcs.155523

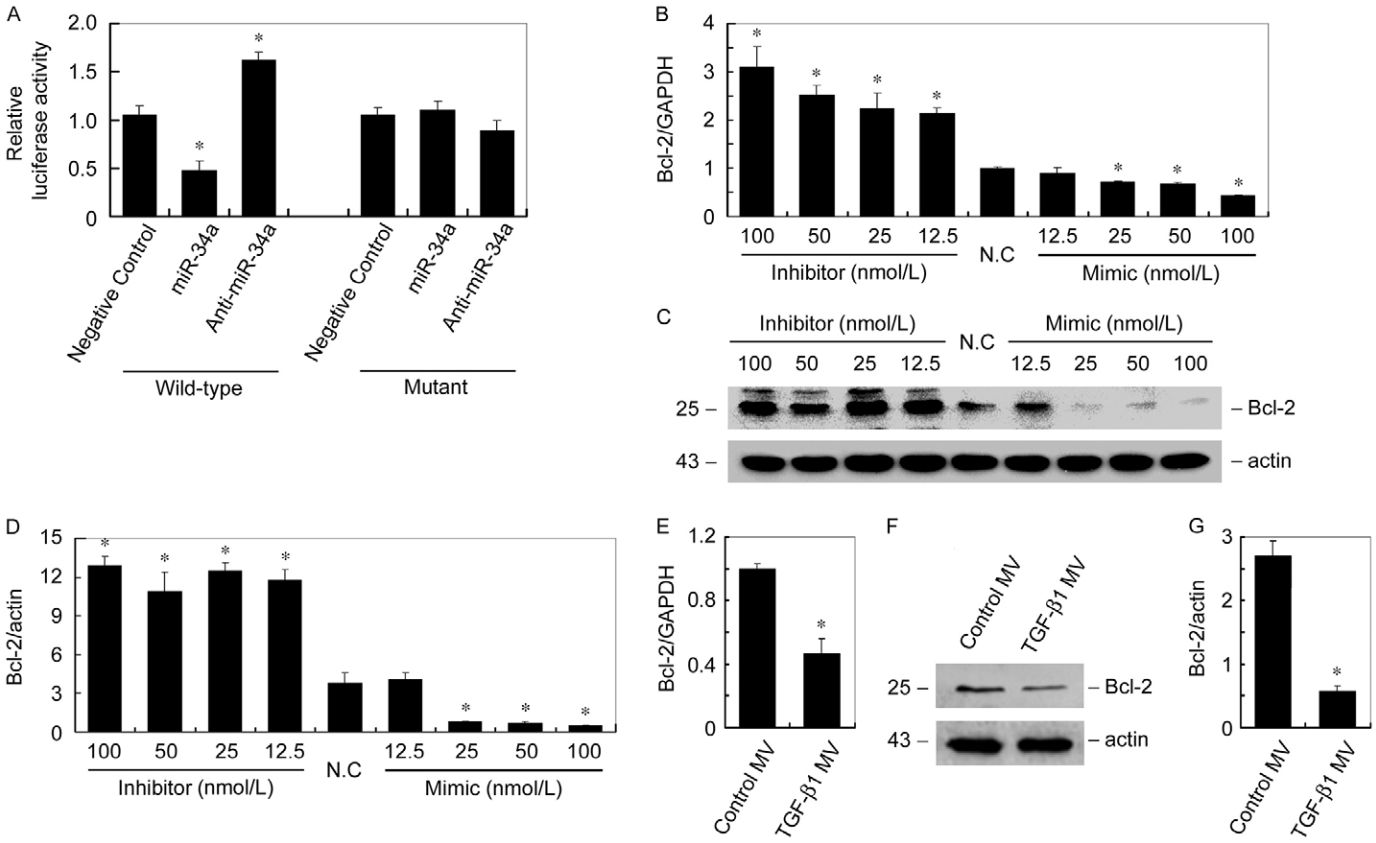

Fig. 5. miR-34a targets anti-apoptotic Bcl-2 in tubular cells. (A) Relative luciferase activity in NRK-52E cells transfected with plasmids as indicated for 24 hours. The data are representative of three experiments. (B) Q-PCR analysis of relative mRNA expression levels of Bcl-2 in NRK-52E cells transfected with miR-34a inhibitor, miR-34a mimic or negative control (N.C.) (C) Western blot analysis of the protein expression levels of Bcl-2 in NRK-52E cells transfected with miR-34a inhibitor, miR-34a mimic or negative control. (D) Graphic representation of relative Bcl-2 abundance normalized to actin. (E) Q-PCR analysis of relative mRNA expression levels of Bcl-2 in NRK-52E cells incubated with control MV (microvesicles, isolated from control NRK-49F cells) or TGF-β1 MV (isolated from TGF-β1-treated NRK-49F cells). (F) Western blot analysis of the protein expression levels of Bcl-2 in NRK-52E cells incubated with control MV or TGF-β1 MV. (G) Graphic representation of relative Bcl-2 abundance normalized to actin. Data in A,B,D,E and G show the mean±s.e.m. (n=3); *P<0.05 versus negative control (A–C) or versus control (E,F).

Apoptosis is one of the reasons for tubular cell loss and proximal tubular atrophy, which ultimately contributes to renal fibrosis. In this study, apoptosis was evident in fibrotic kidney that was induced by UUO. These apoptotic cells became detached from the TBM and were excreted in urine (supplementary material Fig. S1). It has been reported that dysregulation of miR-34 is involved in the development of some cancers because miR-34 regulates cell apoptosis. In mammals, the miR-34 family has three major mature miRNAs, miR-34a, miR-34b and miR-34c. The expression of miR-34a in mouse is observed in all tissues; however, miR-34b and miR-34c are relatively less abundant in most tissues. The mature miR-34a has been demonstrated to be a part of the p53 tumor suppressor network of proteins. We therefore hypothesized that the upregulation of miR-34a was associated with proximal tubular cell apoptosis in renal fibrosis.

Firstly, the expression and localization of miR-34a was determined in fibrotic kidney. As we expected, the expression of miR-34a was markedly upregulated after kidney obstruction, and miR-34a expression was predominantly located in tubular and interstitial cells (Fig. 1). Moreover, the amount of miR-34a in urine from obstructed kidney was very strongly increased. The total RNA level in urine from obstructed kidneys was not increased after UUO (data not shown). miR-34a might be excreted with apoptotic cells into the urine, and it is probably present in the urine in apoptotic cells or cell debris. The excretion of miR-34a into urine might explain the relatively moderate increase in miR-34a in fibrotic kidney (less than threefold).

In obstructed kidney, tubular cells and interstitial fibroblasts are two major parenchymal cell types that contribute to the progression of renal fibrosis. An ISH assay showed that miRNA-34a was localized in tubulointerstitial spaces. The increased excretion of miR-34a into urine was probably a result of the shedding of tubular cells; however, the expression of miR-34a was not upregulated in cultured proximal tubular cells that were incubated with TGF-β1. By contrast, miR-34a was markedly upregulated in TGF-β1-treated fibroblasts (Fig. 2). Moreover, miR-34a in microvesicles isolated from obstructed kidneys was markedly upregulated (Fig. 1). We therefore hypothesized that miR-34a might be transported from fibroblasts to tubular cells. Thus, it was found in this study that tubular cells and fibroblasts function together to induce apoptosis, and are connected by microvesicles. Under normal conditions, tubular cells and fibroblasts are separated by the TBM. However, in fibrotic kidney, the disrupted TBM always provides a route connecting tubular cells and fibroblasts. Recently, Raghu Kalluri et al.

Journal of Cell Science (2014) 127, 4494–4506 doi:10.1242/jcs.155523

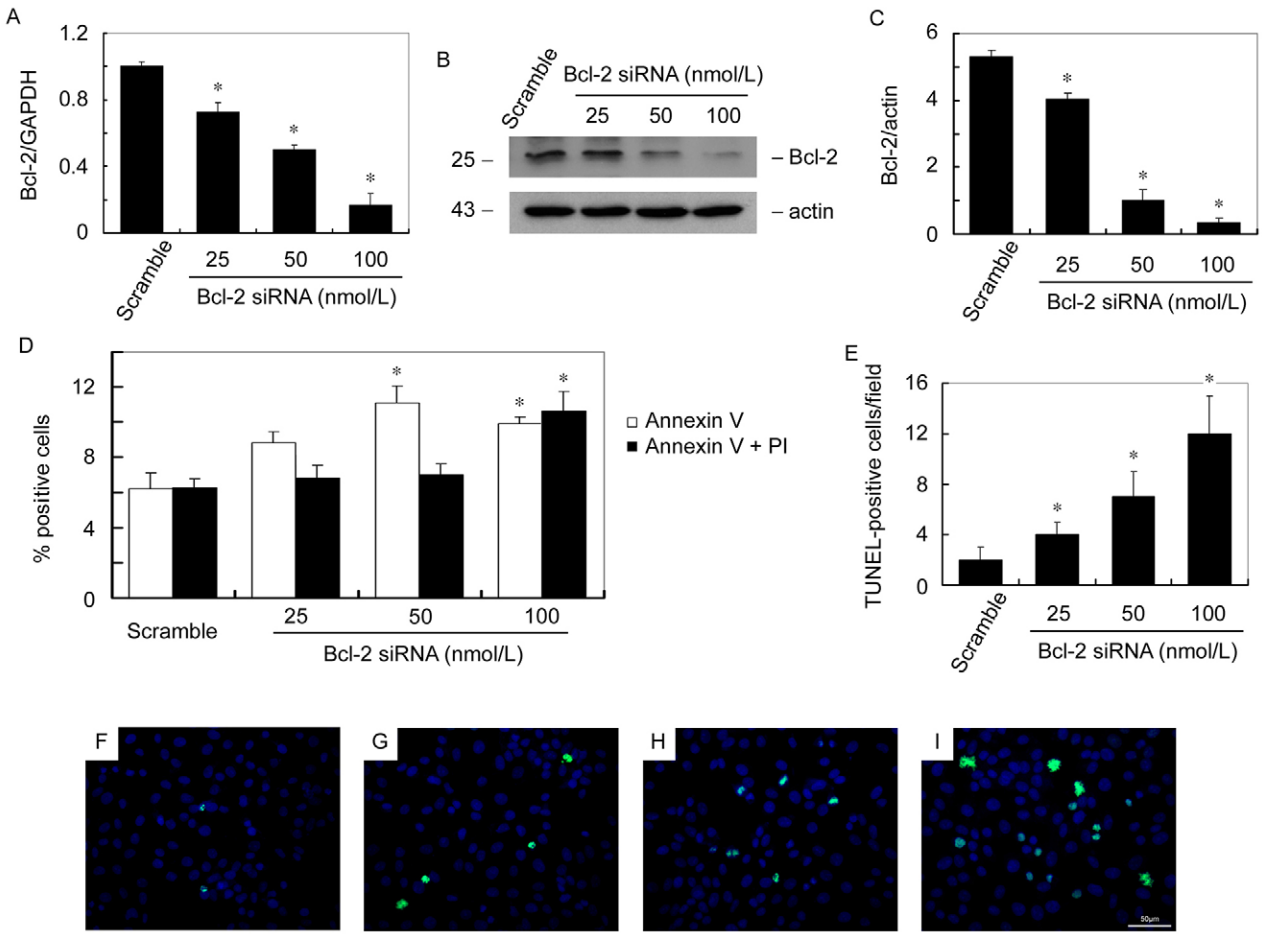

Fig. 6. Downregulation of Bcl-2 results in apoptosis of tubular cells. (A) Q-PCR analysis of relative mRNA expression levels of Bcl-2 in NRK-52E cells transfected with different doses of Bcl-2 siRNA as indicated. (B) Western blot analysis of relative protein expression levels of Bcl-2 in NRK-52E cells transfected with different doses of Bcl-2 siRNA as indicated. (C) Graphic representation of relative Bcl-2 quantity normalized to actin. (D) Graphic representation of the percentage of positive cells as determined by annexin V/propidium iodide (PI) staining on a flow cytometer. (E) Graphic representation of the percentage of positive cells as determined by TUNEL staining. Data in A,C–E show the mean±s.e.m. (n=3); *P<0.05 versus scramble control siRNA. (F–I) Representative images showing the apoptosis of NRK-52E cells incubated with different doses of Bcl-2 siRNA as determined by TUNEL staining. (F) 50 nmol/l scramble control siRNA. (G) 25 nmol/l Bcl-2 siRNA. (H) 50 nmol/l Bcl-2 siRNA. (I) 100 nmol/l of Bcl-2 siRNA. Scale bars: 50 μm.

reported that the mRNA of TGF-β1 could be transported from injured epithelial cells to fibroblasts, which then initiate tissue regeneration and fibrosis (Borges et al., 2013). Thus, the transportation of miRNA between fibroblasts and tubular cells is quite possible.

Because of the presence of RNase in tissue and body fluids, the transportation of naked miRNA seems unlikely. In Kalluri's study, the mRNA of TGF-β1 was transported in exosomes (Borges et al., 2013). In our previous study, miR-21 was packaged into microvesicles and transported between tubular cells, promoting tubular phenotype transition and fibrosis (Zhou et al., 2013). It has already been demonstrated that tumor microvesicles contain protein, mRNA and miRNA that allow them to operate as vectors for short- or long-range delivery of signals to other cells (Martins et al., 2013). Microvesicles seem to be perfect shuttles for miRNA. They are secreted nanoparticles delimited by a lipid bilayer that comes from donor cells. This characteristic was applied to verify the transportability of microvesicles from fibroblasts to tubular cells. The membrane of donor fibroblasts was pre-stained with Dil-C18, a membrane dye (Zhang et al., 2010; Zhou et al., 2013). Once secreted, microvesicles would carry part of the donor membrane and thus would be Dil-C18 positive. These microvesicles were collected by centrifugation and incubated with cultured tubular epithelial cells. The Dil-C18-positive membrane carried by microvesicles would be transported into recipient cells after their fusion or engulfment, which resulted in the detection of Dil-C18 fluorescence in recipient tubular epithelial cells. As we expected, microvesicles were transported into >30% of recipient tubular epithelial cells (Fig. 2). The direct detection of microvesicles by flow cytometry is difficult because of their small size; however, fusion or engulfment of microvesicles by tubular epithelial cells causes the fluorescence to accumulate within the cells, making it easier to detect. In other words, it is likely that a higher percentage of tubular epithelial cells contained microvesicles; however, they could not be detected when they contained relatively few microvesicles.

Because total RNA was isolated from kidney and fibroblast microvesicles that contained 1 mg of microvesicle protein, the observed upregulation of miR-34a indicated that the miR-34a content in each microvesicle was markedly increased after obstruction (Figs 1, 3). CD63 is the protein marker of

Journal of Cell Science (2014) 127, 4494–4506 doi:10.1242/jcs.155523

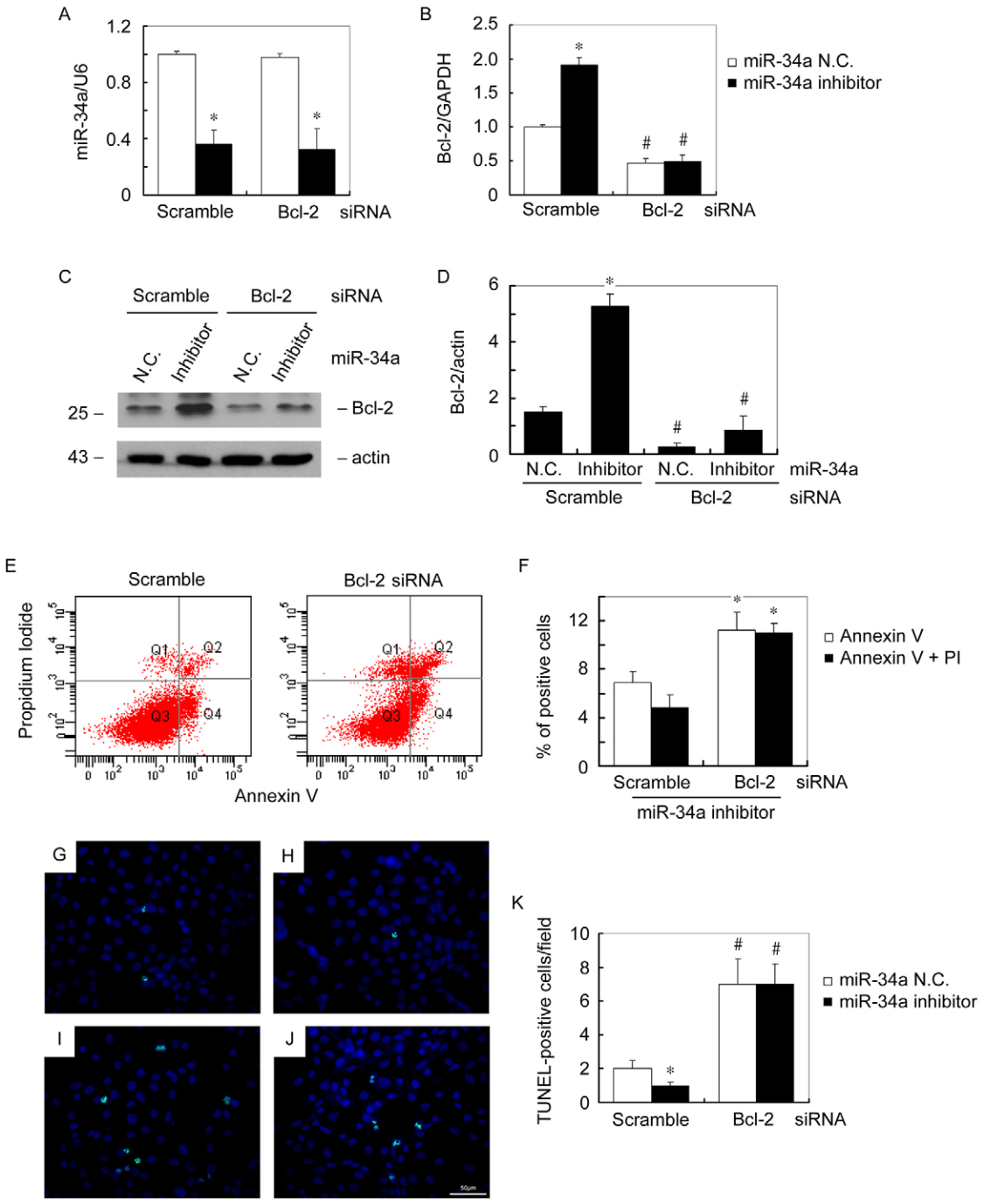

Fig. 7. miR-34a regulates tubular cell apoptosis by targeting Bcl-2. (A) Q-PCR analysis of relative expression levels of miR-34a in NRK-52E cells co-transfected with miR-34a inhibitor (50 nmol/l) and Bcl-2 siRNA (50 nmol/l). (B) Q-PCR analysis of relative mRNA expression levels of Bcl-2 in NRK-52E cells co-transfected with miR-34a inhibitor (50 nmol/l) and Bcl-2 siRNA (50 nmol/l). N.C., negative control. (C) Western blot analysis of protein expression levels of Bcl-2 in NRK-52E cells co-transfected with miR-34a inhibitor (50 nmol/l) and Bcl-2 siRNA (50 nmol/l). (D) Graphic representation of relative Bcl-2 abundance normalized to actin. (E) Apoptosis of NRK-52E cells co-transfected with miR-34a inhibitor and Bcl-2 scramble control siRNA or miR-34a inhibitor and Bcl-2 siRNA was analyzed by annexin V/propidium iodide (PI) staining on a flow cytometer. (F) Graphic representation of the percentage of positive cells as determined by using flow cytometry. (G–J) Representative images show the apoptosis of NRK-52E cells co-transfected with miR-34a inhibitor and Bcl-2 siRNA as determined by TUNEL staining. (G) miR-34a negative control and Bcl-2 scramble control siRNA. (H) miR-34a inhibitor and Bcl-2 scramble control siRNA. (I) miR-34a negative control and Bcl-2 siRNA. (J) miR-34a inhibitor and Bcl-2 siRNA. Scale bars: 50 μm. (K) Graphic representation of the percentage of positive cells as determined by TUNEL staining. Data in A,B,D,F and K show the mean±s.e.m. (n=3); *P<0.05 versus corresponding cells transfected with miR-34a N.C. (A,B,D,K) or versus corresponding cells transfected with Bcl-2 scramble control siRNA (F); $^{\#}P$<0.05 versus corresponding cells transfected with Bcl-2 scramble control siRNA.

Journal of Cell Science (2014) 127, 4494–4506 doi:10.1242/jcs.155523

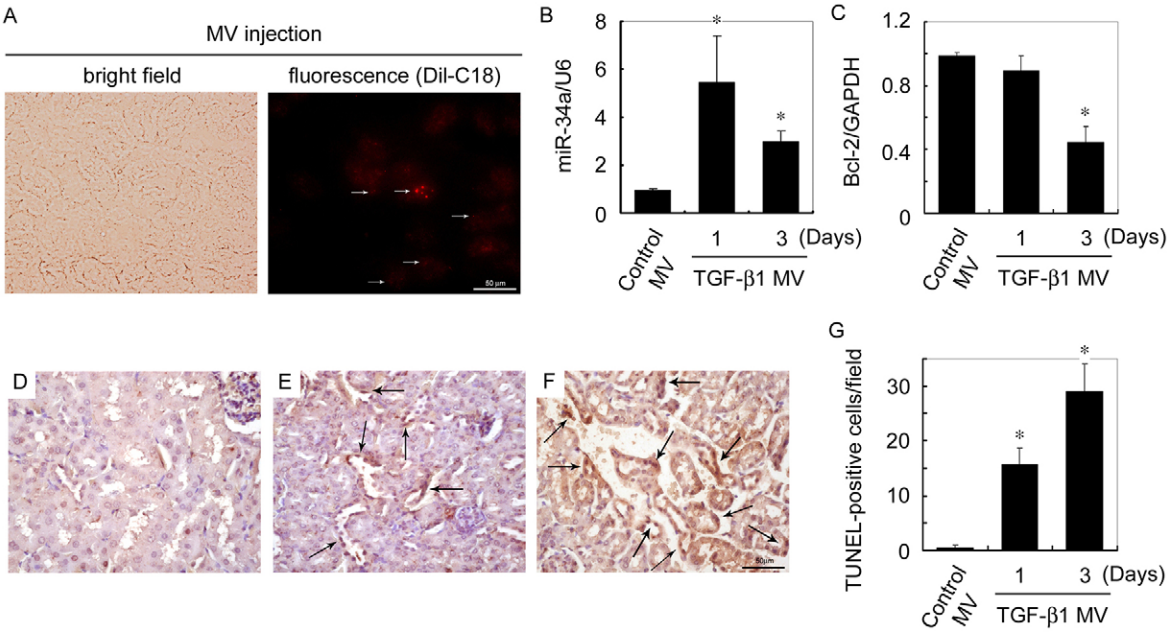

Fig. 8. Exogenous miR-34a-containing microvesicles from TGF-β1-treated fibroblasts enhance tubular cell apoptosis. (A) Representative images show Dil-C18-labeled microvesicles (MV) in mouse kidney at 1 day after intravenous injection. Dil-C18-labeled microvesicles isolated from TGF-β1-treated NRK-49F cells (TGF-β1 MV) were injected through the tail vein into CD-1 mice. After 1 day, the kidney was harvested and kidney sections were viewed by microscopy. (B) Mice were injected with microvesicles isolated from NRK-49F cells incubated without (control MV) or with TGF-β1 (TGF-β1 MV). Q-PCR analysis of relative expression levels of miR-34a in mouse kidney is shown. (C) Q-PCR analysis of relative mRNA expression levels of Bcl-2 in mouse kidney is shown. (D–F) Representative images show apoptosis in kidneys from mice injected with control MV and TGF-β1 MV as determined by TUNEL staining. (D) Kidney of a mouse injected with control MV. (E) Kidney of a mouse injected with TGF-β1 MV at 1 day after injection. (F) Kidney of a mouse injected with TGF-β1 MV at 3 days after injection. Arrows point to TUNEL-positive cells (brown nuclei). Scale bars: 50 μm. (G) Graphic representation of the percentage of positive cells as determined by TUNEL staining. Data in B,C and G show the mean±s.e.m. (n=3); *P<0.05 versus control.

microvesicles. Because protein extracts prepared from kidney and fibroblast microvesicles were normalized to kidney tissue and cell protein level (actin), and the size of microvesicles was within the same range, the upregulated CD63 not only proved that the isolated pellet contained microvesicles but also indicated that obstructed kidneys and TGF-β1-treated fibroblasts produced more microvesicles than controls. However, in obstructed kidneys, the pellet of isolated microvesicles contained all kinds of microvesicles secreted by various types of kidney cells, and the origin of miR-34a was therefore uncertain. It was difficult to directly observe the process of microvesicle secretion in mouse kidney. Microvesicles contain markers of the cells from which they originated; however, it is difficult to investigate the colocalization of protein markers of microvesicles and their miRNA contents in kidney tissue samples. We therefore detected fibroblast microvesicles in cultured cells.

It has been demonstrated that miR-34a regulates apoptosis by targeting Bcl-2 in various tumor cells (Cole et al., 2008; Hu et al., 2013; Ji et al., 2012; Kastl et al., 2012; Liu et al., 2011; Liu, 2010; Mraz et al., 2009; Nalls et al., 2011; Peng et al., 2013; Yang et al., 2013). Here, in cultured proximal tubular cells, the upregulation of miR-34a by microvesicle delivery or mimic transfection induced cell apoptosis, whereas downregulation of miR-34a by inhibitor transfection inhibited apoptosis (Figs 3, 4). The pro-apoptotic activity of miR-34a delivered by microvesicles was proved in cultured tubular cells, and was then further examined in mouse kidney. miR-34a-containing microvesicles were injected through the tail vein. Owing to characteristics of the circulatory system, it is harder for microvesicles to arrive at kidney than at liver and lung. However, immunofluorescently labeled microvesicles were observed in the kidney. This might be explained by the relatively large dose of microvesicles (from $\sim 10^7$ cells per mouse) that we administered. Moreover, microvesicles from fibroblasts might have special proteins in their lipid membrane that help to choose specific target cells. The exogenous miR-34a was successfully delivered into mouse kidney, where it downregulated the expression of Bcl-2 and induced apoptosis of tubular cells (Fig. 8). Moreover, the increase in miR-34a was indeed due to direct delivery of exogenous miRNA from fibroblasts, not because of the transport of the factors stimulating production of the miRNA in the target tubular cell (Fig. 3D; supplementary material Figs S2, S4). Fibroblasts might secrete the upregulated miR-34a in microvesicles to avoid the upregulation of fibroblast apoptosis, which could explain why miR-34a is originally upregulated in fibroblasts but induces apoptosis in tubular cells. The secretion of harmful molecules in microvesicles has been previously reported to be a self-protective strategy of cells (Camussi et al., 1987; Pilzer and Fishelson, 2005). The transport mode of microvesicles administrated intravenously is different from that of microvesicles that travel through the disrupted TBM in obstructed kidney. However, the pro-apoptotic effect of exogenous miR-34a delivered by microvesicles to tubular cells was identical.

In tubular cells, miR-34a induced the degradation of Bcl-2 mRNA (Fig. 5). As an anti-apoptotic protein, Bcl-2 is normally expressed in tubular cells. The downregulation of Bcl-2 by RNA interference resulted in tubular cell apoptosis (Fig. 6), which suggests that Bcl-2 is important for the maintenance of tubular

cell survival. The pro-survival effect of the miR-34a inhibitor was dependent on the upregulation of Bcl-2, which was abolished by Bcl-2 siRNA (Fig. 7). These results confirm that miR-34a regulates the apoptosis of tubular cells by targeting Bcl-2.

The present study extends our understanding of the pathogenesis of tubular cell apoptosis and renal fibrosis by illustrating that miR-34a can be secreted from fibroblasts and delivered into tubular cells, and that this exogenous miR-34a can alter the cellular functions of the recipient cells by modulating the expression of the target gene Bcl-2. Secreted miRNAs might represent a class of signaling molecules that play an important role in mediating cell-to-cell communication. The discovery of microvesicle-mediated miRNA-based cell communication might help us to uncover novel mechanisms of renal disease and to develop new therapeutic strategies.

MATERIALS AND METHODS

Animal models

Male CD-1 mice weighing 18–20 g were purchased from Shanghai Experimental Animal Center (Shanghai, China). They were housed in the animal facilities of the Experimental Animal Center of Nanjing Medical University with free access to food and water. Animals were treated humanely in accordance with National Medical Advisory Committee (NMAC) guidelines and using approved procedures of the Institutional Animal Care and Use committee at the Nanjing Medical University. CD-1 mice were randomly assigned into six groups (with five mice per group) – the sham group and groups with unilateral ureteral obstruction (UUO) for 1, 3, 7, 14 or 28 days. UUO was performed using an established procedure (Yang and Liu, 2001). Briefly, under general anesthesia, complete left ureteral obstruction was performed by double-ligating of the left ureter using 4-0 silk after creating a midline abdominal incision. Mice of the sham group had their ureter exposed and manipulated but not ligated. Mice were killed at different time-points as indicated after surgery, and the obstructed kidneys were removed for further investigation.

Cell culture and treatment

The rat renal fibroblast cell line (NRK-49F) and proximal tubular epithelial cell line (NRK-52E) were purchased from the Cell Resource Center of Shanghai Institutes for Biological Sciences Chinese Academy of Sciences, and were originally obtained from the American Type Culture Collection (ATCC) (CRL-1570/1571™). Cells were cultured in DMEM-F12 supplemented with 10% fetal bovine serum (FBS, Invitrogen). For TGF-β1 treatment, NRK-49F cells were seeded at 80% confluence in complete medium containing 10% FBS. After 24 hours, the cells were changed to serum-free medium and incubated for 16 hours. Then cells were treated with recombinant human TGF-β1 (rhTGF-β1, R&D Systems) at a concentration of 5 ng/ml. The culture media of control and TGF-β1-treated NRK-49F cells were collected 48 hours later for microvesicle isolation. For transfection, miR-34a mimic, miR-34a inhibitor (Qiagen) or Bcl-2 siRNA (Invitrogen) were transfected into cells using Lipofectamine 2000 (Invitrogen) according to the protocol provided by the manufacturer.

Transmission electron microscopy

For conventional transmission electron microscopy (TEM), the microvesicle pellet isolated from obstructed kidney was placed in a droplet of 2.5% glutaraldehyde in PBS buffer and fixed. Samples were rinsed and post-fixed in 1% osmium tetroxide. The samples were then embedded in 10% gelatine, fixed and cut into several blocks (<1 mm^3). The samples were dehydrated in increasing concentrations of alcohol and infiltrated with increasing concentrations of Quetol-812 epoxy resin mixed with propylene oxide. Samples were embedded in pure fresh Quetol-812 epoxy resin and polymerized. Ultrathin sections (100 nm) were cut using a Leica UC6 ultra-microtome and post-stained with uranyl acetate for 10 minutes and with lead citrate for 5 minutes at room temperature before observation in a FEI Tecnai T20 transmission electron microscope, operated at 120 kV.

Morphological assessment

Kidney tissues were immersed in 4% neutral-buffered formaldehyde at 4℃ for 48 hours. The tissues were paraffin-embedded, processed for light microscopy and sectioned at 3 μm in thickness. Sections were then stained with Periodic acid–Schiff (PAS) for general histology. Pictures were taken with a Nikon Eclipse 80i microscope equipped with a digital camera (DS-Ri1, Nikon).

TUNEL staining

Renal cell apoptosis was examined by the TUNEL assay using TdT *in situ* apoptosis detection Kit-DAB/Fluorescein from R&D Systems (4812/0-30-K, Trevigen®) according to the instructions provided by the manufacturer. The slides were mounted with mounting medium and TUNEL-positive nuclei were identified by using a Nikon Eclipse 80i Epi-fluorescence microscope equipped with a digital camera (DS-Ri1, Nikon). For quantification, the number of positively stained nuclei (brown or green) per field was determined. Ten randomly selected fields were counted.

miRNA *in situ* hybridization

The miRNA ISH was performed using mercury LNA™ microRNA ISH optimization kit (Exiqon) for formalin-fixed paraffin embedded kidney samples according to the protocol provided by the manufacturer. Briefly, 10-μm thick sections were prepared, followed by deparaffinization in xylene and ethanol. The slides were incubated with 15 mg/ml proteinase K (Exiqon) for 20 minutes at 37℃. After being washed and dehydrated, the slides were hybridized with double-digoxigenin (DIG)-labeled, LNA™ miR-34a probe, LNA™ scrambled miRNA probe, LNA™ U6 snRNA probe or LNA™ miR-126 probe (positive control) (Exiqon) for 1 hour at 55℃. The slides were washed with saline-sodium citrate (SSC) buffer, and then incubated with blocking solution for 15 minutes, followed by incubation with anti-DIG regent for 60 minutes, alkaline phosphatase substrate for 2 hours at 30℃ and KTBT buffer for two 5-min periods. The slides were mounted with mounting medium and analyzed by light microscopy (Nikon Eclipse 80i).

Quantitative PCR analysis of miRNA and mRNA

Quantitative polymerase chain reaction (Q-PCR) was performed using an Applied Biosystems 7300 Sequence Detection system. Total RNA of cells or tissues was prepared using a TRIzol isolation system according to the instructions provided by the manufacturer (Invitrogen). For miRNA cDNA library preparation, the first strand of cDNA was synthesized using 1 μg of RNA in 20 μl of reaction buffer using miScript RT II buffer (Qiagen). The mix was incubated at 37℃ for 60 minutes, followed by 95℃ for 5 minutes. Subsequently, real-time quantification was performed. The 20 μl reaction consisted of 1 μl of cDNA, 2 μl of 10× miScript universal primer, 2 μl of 10× miScript primer Assay, 10 μl of 2× QuantiTect SYBR green PCR Master Mix and RNase-free water (Qiagen). The mixtures were incubated at 95℃ for 15 minutes, followed by 40 cycles of 94℃ for 15 seconds, 55℃ for 30 seconds and 70℃ for 34 seconds. All reactions were run in triplicate. Ct data were determined using default threshold settings and the mean C_t was calculated from the triplicate PCRs. The ratio of miRNAs was calculated by using the equation $2^{-\Delta Ct}$, in which $\Delta Ct = Ct_{treatment} - Ct_{sham/control}$. All primers were purchased from Qiagen. U6 was used for normalization in miRNA Q-PCR when total RNA was extracted from cell or tissue samples. For mRNA cDNA library, the first strand of cDNA was synthesized using 1 μg of RNA in 20 μl of reaction buffer using MLV-RT (Promega, Madison, WI) and random primers at 42℃ for 30 minutes. Quantitative polymerase chain reaction (Q-PCR) was performed using an Applied Biosystems 7300 Sequence Detection system. The Ct data were determined using default threshold settings and the mean Ct was determined from the duplicate PCRs. The ratios to control group were calculated by using the equation $2^{-\Delta Ct}$, in which $\Delta Ct = Ct_{sample} - Ct_{control}$. All the primers were acquired from Qiagen.

Urine collection and RNA isolation

Urine samples from obstructed kidneys and sham-treated kidneys were collected at different time-points as indicated. Urine from obstructed

kidneys was collected from the renal pelvis when mice were killed. An equal volume of 200 µl urine from each group was used for total RNA isolation; acidic phenol was used, followed by chloroform/isopropanol purification. The quantity of total RNA was then determined and normalized. A total of 1 µg of RNA was applied for reverse transcription to create a urine miRNA cDNA library, using miScript II RT kit (Qiagen) in 20 µl of reaction buffer. The mix was incubated at 37℃ for 60 minutes, followed by 95℃ for 5 minutes. Subsequently, real-time quantification was performed as described above.

Immunofluorescent staining

Indirect immunofluorescent staining was performed according an established procedure (Yang and Liu, 2001). Briefly, kidney sections were washed twice with cold PBS and fixed with cold methanol:acetone (1:1) for 10 minutes at −20℃. Following three extensive washings with PBS, the sections were blocked with 0.1% Triton X-100 and 2% normal donkey serum in PBS buffer for 40 minutes at room temperature and then incubated with the anti-laminin antibody (L9393, Sigma-Aldrich), followed by staining with FITC-conjugated secondary antibody. Cells were double-stained with DAPI to visualize the nuclei. Slides were viewed with a Nikon Eclipse 80i Epi-fluorescence microscope equipped with a digital camera (DS-Ri1, Nikon). In each experimental setting, immunofluorescence images were captured with identical exposure settings.

Microvesicle isolation

Microvesicles were isolated from kidney and cell culture medium by differential centrifugation as described previously (Zhang et al., 2010). The kidney cortex was collected and subjected to mechanical and enzymatic digestion with collagenase and trypsin as described previously (Borges et al., 2013). The collected digested tissue and cell culture medium were centrifuged as follows. After removing cells and other debris by centrifugation at 300 ***g***, 1200 ***g*** and 10,000 ***g*** for 5 minutes, 20 minutes and 30 minutes, respectively, the supernatant was centrifuged at 110,000 ***g*** for 1 hour (all steps were performed at 4℃). Microvesicles were collected from the pellet and resuspended in FBS-free media. These microvesicles were applied to NRK-52E cells or administered to mice through the tail vein. Total RNA of microvesicles derived from cells was then extracted using Trizol LS regent (Invitrogen) to examine the miR-34a level. For normalization, the protein concentration of isolated kidney microvesicles was examined. Total RNA of microvesicles derived from kidney was extracted from microvesicle samples containing 1 mg of microvesicle protein.

Fluorescent labeling of microvesicles and quantification of fluorescence-positive cells by flow cytometry

NRK-49F cells were labeled with or without (control) Dil-C18 (a gift from professor Chen-yu Zhang of Nanjing University, China) for 1 hour and then washed three times with PBS. After TGF-β1 treatment, microvesicles were harvested from the cell culture media of control or Dil-C18-labeled NRK-49F cells as described above. Microvesicles were resuspended and applied to cultured NRK-52E cells for 12 hours. Then, some NRK-52E cells were washed, fixed and observed under a Nikon Eclipse 80i Epi-fluorescence microscope equipped with a digital camera (DS-Ri1, Nikon). In each experimental setting, immunofluorescence images were captured with identical exposure settings. Other cells were collected, washed and resuspended. The percentage of fluorescence-positive cells was immediately determined by using a flow cytometer.

For tail vein injection, microvesicles were harvested from cell culture media of control or TGF-β1-treated NRK-49F cells. Microvesicles were resuspended and administered through the tail vein. Each mouse was injected with microvesicles from ~10^7 cells. Kidney, liver and lung were harvested 24 hours after microvesicle administration. The frozen tissues were embedded in optimum cutting temperature compound (OCT) and sectioned at 5 µm in thickness. Microvesicles were identified by using a Nikon Eclipse 80i Epi-fluorescence microscope equipped with a digital camera (DS-Ri1, Nikon).

Luciferase assay

The plasmids of Bcl-2 3′ UTR-wild-type, Bcl-2 3′ UTR-mutant, negative control, miR-34a and anti-miR-34a were constructed by Invitrogen. For miRNA plasmids, the vector was pcDNA6.2-GW/EmGFP-miR (Life, K4936-00). For 3′UTR plasmids, the vector was pmirGLO and the length of inserted sequence was 207 base pairs, containing wild-type or mutant Bcl-2 3′UTR. For the luciferase reporter assay, plasmids were transfected into cells as indicated. At 24 hours after transfection, luciferase activities were measured by using the luciferase reporter assay system (E1980, Promega) and were normalized to that of the negative control group.

Western immunoblot analysis

Samples were lysed with sodium dodecyl sulfate (SDS) sample buffer. The supernatants were collected after centrifugation at 13,000 ***g*** at 4℃ for 20 minutes. Protein concentration was determined using a bicinchoninic acid (BCA) protein assay kit (Sigma), and lysates were mixed with an equal amount of 2× SDS loading buffer. Samples were heated at 100℃ for ~5–10 minutes before loading and were separated on precasted 10% or 5% SDS-polyacrylamide gels (Bio-Rad). Samples with 50 µg protein were loaded in each lane. Detection of protein expression by western blotting was performed as described previously (Yang and Liu, 2001). The primary antibodies were anti-Bcl-2 (2870, Cell Signaling Technology), anti-CD63 (sc-15363, Santa Cruz) and anti-actin (sc-1616, Santa Cruz). Quantification was performed by measurement of the intensity of the signals with the use of National Institutes of Health Image analysis software.

Annexin-V–FITC apoptosis assay

Apoptotic cells were detected using an annexin-V–FITC apoptosis detection kit (Sigma-Aldrich) on a flow cytometer. Briefly, control or treated cells were collected, washed and resuspended in 500 µl of binding buffer at a concentration of ~10^5–10^6 cells/ml. Cells were then stained with annexin-V–FITC and propidium iodide in the dark at room temperature for exactly 10 minutes. The fluorescence of cells was immediately determined by flow cytometry. Live cells showed no staining, early apoptotic cells showed annexin V staining and necrotic cells showed both annexin V and propidium iodide staining.

Statistical analysis

Animals were randomly assigned to control and treatment groups. Statistical analysis was performed using SigmaStat software (Jandel Scientific Software). Comparisons between groups were made using one-way ANOVA, followed by Student's *t*-test. $P<0.05$ was considered significant.

Acknowledgements

We thank professor Chen-yu Zhang of Nanjing University for providing Dil-C18.

Competing interests

The authors declare no competing interests.

Author contributions

J.Y. designed the experiments; J.Y., C.D., K.Z. and Q.S. interpreted the data; Y.Z. and J.Y. wrote the article; and Y.Z., M.X., J.N. and W.S. performed the experiments.

Funding

This work was supported by the '973' Science Program of the Ministry of Science and Technology of China [grant number 2012CB517603]; and the National Science Foundation of China [grant number 31200870].

Supplementary material

Supplementary material available online at
http://jcs.biologists.org/lookup/suppl/doi:10.1242/jcs.155523/-/DC1

References

Bohle, A., Christ, H., Grund, K. E. and Mackensen, S. (1979). The role of the interstitium of the renal cortex in renal disease. *Contrib. Nephrol.* **16**, 109-114.
Bommer, G. T., Gerin, I., Feng, Y., Kaczorowski, A. J., Kuick, R., Love, R. E., Zhai, Y., Giordano, T. J., Qin, Z. S., Moore, B. B. et al. (2007). p53-mediated

activation of miRNA34 candidate tumor-suppressor genes. *Curr. Biol.* **17**, 1298-1307.

Borges, F. T., Melo, S. A., Özdemir, B. C., Kato, N., Revuelta, I., Miller, C. A., Gattone, V. H., I. I, LeBleu, V. S. and Kalluri, R. (2013). TGF-β1-containing exosomes from injured epithelial cells activate fibroblasts to initiate tissue regenerative responses and fibrosis. *J. Am. Soc. Nephrol.* **24**, 385-392.

Budhram-Mahadeo, V., Morris, P. J., Smith, M. D., Midgley, C. A., Boxer, L. M. and Latchman, D. S. (1999). p53 suppresses the activation of the Bcl-2 promoter by the Brn-3a POU family transcription factor. *J. Biol. Chem.* **274**, 15237-15244.

Camussi, G., Salvidio, G., Biesecker, G., Brentjens, J. and Andres, G. (1987). Heymann antibodies induce complement-dependent injury of rat glomerular visceral epithelial cells. *J. Immunol.* **139**, 2906-2914.

Camussi, G., Deregibus, M. C., Bruno, S., Cantaluppi, V. and Biancone, L. (2010). Exosomes/microvesicles as a mechanism of cell-to-cell communication. *Kidney Int.* **78**, 838-848.

Cocucci, E., Racchetti, G., Rupnik, M. and Meldolesi, J. (2008). The regulated exocytosis of enlargeosomes is mediated by a SNARE machinery that includes VAMP4. *J. Cell Sci.* **121**, 2983-2991.

Cole, K. A., Attiyeh, E. F., Mosse, Y. P., Laquaglia, M. J., Diskin, S. J., Brodeur, G. M. and Maris, J. M. (2008). A functional screen identifies miR-34a as a candidate neuroblastoma tumor suppressor gene. *Mol. Cancer Res.* **6**, 735-742.

Dai, C., Yang, J. and Liu, Y. (2003). Transforming growth factor-beta1 potentiates renal tubular epithelial cell death by a mechanism independent of Smad signaling. *J. Biol. Chem.* **278**, 12537-12545.

Docherty, N. G., O'Sullivan, O. E., Healy, D. A., Fitzpatrick, J. M. and Watson, R. W. (2006). Evidence that inhibition of tubular cell apoptosis protects against renal damage and development of fibrosis following ureteric obstruction. *Am. J. Physiol.* **290**, F4-F13.

Gao, X., Mae, H., Ayabe, N., Takai, T., Oshima, K., Hattori, M., Ueki, T., Fujimoto, J. and Tanizawa, T. (2002). Hepatocyte growth factor gene therapy retards the progression of chronic obstructive nephropathy. *Kidney Int.* **62**, 1238-1248.

Hermeking, H. (2010). The miR-34 family in cancer and apoptosis. *Cell Death Differ.* **17**, 193-199.

Hu, Q. L., Jiang, Q. Y., Jin, X., Shen, J., Wang, K., Li, Y. B., Xu, F. J., Tang, G. P. and Li, Z. H. (2013). Cationic microRNA-delivering nanovectors with bifunctional peptides for efficient treatment of PANC-1 xenograft model. *Biomaterials* **34**, 2265-2276.

Ji, X., Wang, Z., Geamanu, A., Goja, A., Sarkar, F. H. and Gupta, S. V. (2012). Delta-tocotrienol suppresses Notch-1 pathway by upregulating miR-34a in nonsmall cell lung cancer cells. *Int. J. Cancer* **131**, 2668-2677.

Johnson, A. and DiPietro, L. A. (2013). Apoptosis and angiogenesis: an evolving mechanism for fibrosis. *FASEB J.* **27**, 3893-3901.

Kastl, L., Brown, I. and Schofield, A. C. (2012). miRNA-34a is associated with docetaxel resistance in human breast cancer cells. *Breast Cancer Res. Treat.* **131**, 445-454.

Kellner, D., Chen, J., Richardson, I., Seshan, S. V., El Chaar, M., Vaughan, E. D., Jr, Poppas, D. and Felsen, D. (2006). Angiotensin receptor blockade decreases fibrosis and fibroblast expression in a rat model of unilateral ureteral obstruction. *J. Urol.* **176**, 806-812.

Kumamoto, K., Spillare, E. A., Fujita, K., Horikawa, I., Yamashita, T., Appella, E., Nagashima, M., Takenoshita, S., Yokota, J. and Harris, C. C. (2008). Nutlin-3a activates p53 to both down-regulate inhibitor of growth 2 and up-regulate mir-34a, mir-34b, and mir-34c expression, and induce senescence. *Cancer Res.* **68**, 3193-3203.

Liu, Y. (2004). Hepatocyte growth factor in kidney fibrosis: therapeutic potential and mechanisms of action. *Am. J. Physiol.* **287**, F7-F16.

Liu, Y. (2010). New insights into epithelial-mesenchymal transition in kidney fibrosis. *J. Am. Soc. Nephrol.* **21**, 212-222.

Liu, C., Zhou, C., Gao, F., Cai, S., Zhang, C., Zhao, L., Zhao, F., Cao, F., Lin, J., Yang, Y. et al. (2011). MiR-34a in age and tissue related radio-sensitivity and serum miR-34a as a novel indicator of radiation injury. *Int. J. Biol. Sci.* **7**, 221-233.

Lodygin, D., Tarasov, V., Epanchintsev, A., Berking, C., Knyazeva, T., Körner, H., Knyazev, P., Diebold, J. and Hermeking, H. (2008). Inactivation of miR-34a by aberrant CpG methylation in multiple types of cancer. *Cell Cycle* **7**, 2591-2600.

Martins, V. R., Dias, M. S. and Hainaut, P. (2013). Tumor-cell-derived microvesicles as carriers of molecular information in cancer. *Curr. Opin. Oncol.* **25**, 66-75.

Miyajima, A., Chen, J., Lawrence, C., Ledbetter, S., Soslow, R. A., Stern, J., Jha, S., Pigato, J., Lemer, M. L., Poppas, D. P. et al. (2000). Antibody to transforming growth factor-beta ameliorates tubular apoptosis in unilateral ureteral obstruction. *Kidney Int.* **58**, 2301-2313.

Mizuno, S., Matsumoto, K. and Nakamura, T. (2001). Hepatocyte growth factor suppresses interstitial fibrosis in a mouse model of obstructive nephropathy. *Kidney Int.* **59**, 1304-1314.

Morrissey, J., Hruska, K., Guo, G., Wang, S., Chen, Q. and Klahr, S. (2002). Bone morphogenetic protein-7 improves renal fibrosis and accelerates the return of renal function. *J. Am. Soc. Nephrol.* **13 Suppl. 1**, S14-S21.

Mraz, M., Pospisilova, S., Malinova, K., Slapak, I. and Mayer, J. (2009). MicroRNAs in chronic lymphocytic leukemia pathogenesis and disease subtypes. *Leuk. Lymphoma* **50**, 506-509.

Nalls, D., Tang, S. N., Rodova, M., Srivastava, R. K. and Shankar, S. (2011). Targeting epigenetic regulation of miR-34a for treatment of pancreatic cancer by inhibition of pancreatic cancer stem cells. *PLoS ONE* **6**, e24099.

Peng, X., Shao, J., Shen, Y., Zhou, Y., Cao, Q., Hu, J., He, W., Yu, X., Liu, X., Marian, A. J. et al. (2013). FAT10 protects cardiac myocytes against apoptosis. *J. Mol. Cell. Cardiol.* **59**, 1-10.

Pilzer, D. and Fishelson, Z. (2005). Mortalin/GRP75 promotes release of membrane vesicles from immune attacked cells and protection from complement-mediated lysis. *Int. Immunol.* **17**, 1239-1248.

Théry, C., Zitvogel, L. and Amigorena, S. (2002). Exosomes: composition, biogenesis and function. *Nat. Rev. Immunol.* **2**, 569-579.

Yang, J. and Liu, Y. (2001). Dissection of key events in tubular epithelial to myofibroblast transition and its implications in renal interstitial fibrosis. *Am. J. Pathol.* **159**, 1465-1475.

Yang, F., Li, Q. J., Gong, Z. B., Zhou, L., You, N., Wang, S., Li, X. L., Li, J. J., An, J. Z., Wang, D. S. et al. (2013). MicroRNA-34a Targets Bcl-2 and Sensitizes Human Hepatocellular Carcinoma Cells to Sorafenib Treatment. *Technol. Cancer Res. Treat*.

Zhang, G., Oldroyd, S. D., Huang, L. H., Yang, B., Li, Y., Ye, R. and El Nahas, A. M. (2001). Role of apoptosis and Bcl-2/Bax in the development of tubulointerstitial fibrosis during experimental obstructive nephropathy. *Exp. Nephrol.* **9**, 71-80.

Zhang, Y., Liu, D., Chen, X., Li, J., Li, L., Bian, Z., Sun, F., Lu, J., Yin, Y., Cai, X. et al. (2010). Secreted monocytic miR-150 enhances targeted endothelial cell migration. *Mol. Cell* **39**, 133-144.

Zhou, Y., Xiong, M., Fang, L., Jiang, L., Wen, P., Dai, C., Zhang, C. Y. and Yang, J. (2013). miR-21-containing microvesicles from injured tubular epithelial cells promote tubular phenotype transition by targeting PTEN protein. *Am. J. Pathol.* **183**, 1183-1196.